

Seed-bank contribution in maintaining phytoplanktonic biodiversity

May 20, 2020

Introduction

How the high biodiversity of plant communities maintains is still an unresolved question for both experimental and theoretical ecology. Terrestrial plants and phytoplanktonic communities can present hundreds of species relying on similar resources. Early theory has proposed that environmental fluctuations only [ref] could sustain coexistence but further research showed that this could not explain the order of magnitude of species richness [ref]. Other mechanisms such as niche differentiation [ref], demography [ref] and life history traits [ref] have completed explanation by the stochastic environmental variations and demographic processes.

Analyses of coexistence in terrestrial plant communities often take into account several life stages [refs cf. Adler paper]. Considering at least two stages, seeds/juveniles and adults, different models have uncovered mechanisms that might explain long-term coexistence. Examples of such mechanisms are bet-hedging, the storage effect and the Janzen-Connell effect. Bet-hedging is a long-term strategy relying on the creation of seeds which can remain dormant for a long period of time (over a year, often much longer). Dormant seeds can tolerate harsher years during which adults cannot maintain, but they also reduce part of the population that could germinate from one year to another (in case of an annual plant). The storage effect has first been defined by the presence of a long-lived life stage and temporal variation in recruitment from this long-lived life stage that helps escape interspecific competition (Chesson, 1986; Cáceres, 1997). This has been later generalized as a negative correlation between the effect of the environment and the effect of competition (Ellner *et al.*, 2016). In good environmental conditions, competition between individuals is stronger as seeds might germinate and therefore use the same resources at the same time. Finally, models and experiments suggest that adults can have a negative effect on seed survival, through the Janzen-Connell effect (Comita *et al.*, 2014). Therefore, neglecting explicit modeling of this life stage can modify the understanding we have of the dynamics of the populations (Nguyen *et al.*, 2019).

Even though different coexistence mechanisms have been unveiled through the use of several life stages and a focus on the youngest stage (seeds) for terrestrial plants, the life cycle of aquatic plants, and more specifically that of phytoplanktonic algae, have not been modeled with the same attention. Although ecologists have proposed for a long time that the blooms (peaks in abundances that can cover several orders of magnitude) may initiate after the resuspension and germination of phytoplanktonic resting cells, cysts, (Patrick, 1948; Marcus & Boero, 1998), it is unusual to see an explicit model of such process (but see Hinners *et al.*, 2019). The classical view behind phytoplankton dynamics is that bloom formation is mostly seasonal, due to the variation in light and temperature, assuming vegetative cells remaining in the environment can duplicate enough to attain bloom amplitude. However, a recent review (Ellegaard & Ribeiro, 2018) suggests that cysts might be another player.

Phytoplankton communities in coastal environments may benefit from seed banks (hereafter called cyst banks to remain consistent with phytoplankton terminology) even more than the oceanic communities [REF-find back], as the distance to the sea bottom is smaller allowing recolonization of the pelagic environment from the shallow sea

bottom. In the open sea, cysts might arrive together with animals, but such events might be rarer in comparison. Also, and similarly to the seed bank approach in the terrestrial plant literature, Smayda (2002) has proposed the term “pelagic seed bank” to characterize the contribution of the ocean to coastal communities. This has been noticed for dinoflagellates especially [[ref Dinophysis, check what we have on diatoms]]. Conversely, in many other bloom-forming species the nutrient-rich coastal areas might function as a reservoir for the biodiversity in the ocean, especially in the long run. Indeed, cysts are able to germinate again after dozens of years (McQuoid *et al.*, 2002; Ellegaard & Ribeiro, 2018) or even thousands of years (Sanyal *et al.*, 2018) of dormancy, so they can have a long-term effect on biodiversity in both oceanic and coastal environments.

Here we build on multiple studies in plant and plankton ecology to investigate the effects of cyst banks on phytoplankton community dynamics. XXX [and we describe a little less the models and a little more what we do / what we find, which we can do later]

Methods

Models

Our models builds atop those developed by Shoemaker & Melbourne (2016) and Wisnoski *et al.* (2019) These discrete-time models are designed for metacommunities with multiple competing populations and unfold as follow: first, populations grow or decline according to a Beverton-Holt (BH) multispecies density-dependence (eqs. 1 and 3), and then, in a second step, exchanges occur between the different compartments or patches constituting the metacommunity (eq. 4).

In this paper, individuals are phytoplanktonic cells that move between the upper layer of coastal water, its bottom layer where a cyst bank accumulates and the ocean. Only oceanic and coastal pelagic cells are subject to BH-density dependence. Cysts are only affected by mortality m and burial due to sedimentation ζ . The different populations are field-inspired morphotypes accounting for the most frequent genera observed along the French coast (Picoche & Barraquand, 2020) and will hereafter be called taxa. Parameters and state variables are defined in Table 1.

The BH formulation of multispecies population dynamics is a Lotka-Volterra competition equivalent for discrete-time models, and is often used to represent terrestrial plant population/community dynamics. In this model, the maximum achievable growth rate is modified by both competitive and facilitative interactions, which translates into positive and negative α_{ij} coefficients respectively. We first use the classical multispecies Beverton-Holt model (model I, eq. 1). We subsequently defined saturating interactions (model II, eq. 3). More specifically, in our case, the first step of the first model is written as

$$\begin{cases} N_{t',i,c} &= \frac{\exp(r_i(T))N_{t,i,c}}{1+\sum_j \alpha_{ij}N_{t,j,c}} - lN_{t,i,c} \\ N_{t',i,o} &= \frac{\exp(r_i(T))N_{t,i,o}}{1+k_{c2o}\sum_j \alpha_{ij}N_{t,j,o}} - lN_{t,i,o} \\ N_{t',i,b} &= N_{t,i,b}(1-m-\zeta) \end{cases} \quad (1)$$

where the intrinsic growth rate $r_i(T)$ is a taxon-specific function of the temperature (see eq. 2), the interaction coefficients α_{ij} are the strength of the effect of species j on species i , and the loss term l accounts for lethal processes such a natural mortality, predation or parasitism. First estimate of interaction coefficients are inferred from our previous work on coastal data with Multivariate AutoRegressive (MAR) models (Picoche & Barraquand, 2020). How to shift from MAR- to BH-interaction matrices is described in the SI. We later calibrate this coefficient to an empirical dataset, since MAR models were applied at a different timescale.

In model I, we assume that competition for nutrients is stronger in the ocean than along the coast [ref], thus a coefficient $k_{c2o} > 1$ is applied to competitive interactions.

The growth rate $r_i(T)$ is a modified version of the formula by Scranton & Vasseur (2016) (eq. 2).

$$\begin{aligned}
r_i(T) &= E(T)f_i(T) \\
\text{where } E(T) &= d \times 0.81e^{0.0631T_{\circ c}} \\
\text{and } f_i(T) &= \begin{cases} \exp(-|T_K - T_{K,i}^{opt}|^3/b_i), & T_K \leq T_{K,i}^{opt} \\ \exp(-5|T_K - T_{K,i}^{opt}|^3/b_i), & T > T_{K,i}^{opt} \end{cases}
\end{aligned} \tag{2}$$

where $r_i(T)$ can be decomposed in two parts: the taxon-independent metabolism part $E(T)$ and the taxon-specific niche part $f_i(T)$. The metabolism part describes the maximum achievable growth rate based on Bissinger *et al.* (2008), as an update of the formula by Eppley (1972) used in Scranton & Vasseur (2016). This maximum daily growth rate is weighted by the daylength d as no growth occurs at night. The niche part $f_i(T)$ describes the decrease in growth rate due to the difference between the temperature in the environment and the taxon-specific thermal optimum $T_{K,i}^{opt}$, and is controlled by the specific thermal decay b_i which depends of the niche width. Parameterisation is detailed in the SI.

In model II, oceanic and coastal dynamics are governed by eq. 2.

$$N_{t',i,c/o} = \frac{\exp(r_i(T))N_{t,i,c/o}}{1 + \sum_{j \in \mathbb{C}} \frac{a_C N_{t,j,c/o}}{H_{ij} + N_{t,j,c/o}} + \sum_{j \in \mathbb{F}} \frac{a_F N_{t,j,c/o}}{H_{ij} + N_{t,j,c/o}}} - lN_{t,i,c/o} \tag{3}$$

where a_C and a_F are the maximum competition and facilitation strengths, respectively, with \mathbb{C} and \mathbb{F} the sets of competitors and facilitators of taxon i . We use here similar notations to Qian & Akçay (2020), but have different parameters that vary between species. Indeed, the half-saturation coefficients H_{ij} are here variable between species, since it did not make sense biologically for this quantity to be fixed (e.g., in a resource competition context, different species are expected to feel resource limitations at different concentrations of nutrients and at different number of competitors). . How to use parameter estimates from model I to specify model II is described in the SI.

After growth and mortality happen, exchanges take place between the three compartments during the second step of the model (eq. 4).

$$\begin{cases} N_{t+1,i,c} &= (1 - s_i - e)N_{t',i,c} + \gamma N_{t',i,b} + eN_{t',i,o} \\ N_{t+1,i,o} &= (1 - s_i - e)N_{t',i,o} + eN_{t',i,c} \\ N_{t+1,i,b} &= (1 - \gamma)N_{t',i,b} + s_i N_{t',i,c} \end{cases} \tag{4}$$

Param	Name	Value (unit)	Status
$N_{t,i,c/o/b}$	Abundance of taxon i at time t in the coast (c) or ocean (o), or in the coastal benthos (b)	NA (Number of cells)	Dynamic
$T_{K/^{\circ}C}$	Temperature	NA ($K/^{\circ}C$)	Dynamic
$r_i(T)$	Growth rate of taxon i	NA	Dynamic
b_i	Thermal decay	Field-based, taxon-specific (K^3)	Calibrated
T_i^{opt}	Optimal temperature for taxon i	Field-based, taxon-specific (K)	Calibrated
d	Daylength	0.5 (%)	Fixed
$\alpha_{i,j,c/o}$	Interaction strength of taxon j on i in model I	Field-based, taxon-specific (Cells^{-1})	Calibrated
k_{c2o}	Ocean/Coast interaction strength ratio in model I	1.5	Fixed
a_C/a_F	Maximum competitive/facilitative interaction strength in model II	Field-based, taxon-specific (NA)	Calibrated
H_{ij}	Half-saturation for the interaction strength of taxon j on i in model II	Field-based, taxon-specific (Cells)	Calibrated
s_i	Sinking rate of taxon i	$\{0.1; \mathbf{0.3}; 0.5\}\beta(0.55, 1.25)$	Fixed
e	Exchange rate between ocean and coast	0.4; 0 in scenario	Scenario
l	Loss rate of vegetative phytoplanktonic cells	0.04; 0.1; $\mathbf{0.2}$	Fixed
m	Cyst mortality rate	$\approx 10^{-4}/\mathbf{10^{-5}}$; $1 - \zeta$ in scenario	Scenario
ζ	Cyst burial rate	$10^{-3}, \mathbf{10^{-2}}, 10^{-1}$	Fixed
γ	Germination \times Resuspension rate	$10^{-3}, \mathbf{10^{-2}}, 10^{-1} \times 10^{-5}, 10^{-3}, \mathbf{10^{-1}}$	Fixed

Table 1: Definition of main state variables and parameters of the models. Calibrated parameters are either directly estimated on data for this study or parameters for which initial estimates exist, but are improved through calibration. Fixed values or distributions are estimated from the literature and references are given in the main text. When a range of values is given, the bold numbers indicate the reference values while the others are used to test the sensitivity of the model. Scenario parameters are the parameters which are used to build ecological scenarii.

Each compartment (ocean, coast, seed bank) contains 10^3 cells at the beginning of the simulation, and is run for 1000 time steps. .

Parameterisation

Empirical dataset used for calibration

[[Write here]]

Parameter definition and values

Loss rate The loss rate of vegetative cells can be attributed to natural mortality, predation or parasitism. A maximum value of 0.2 is fixed for the model.

Sinking rate Phytoplanktonic particles have a higher density than water and cannot swim to prevent sinking (although see Reynolds (2006) for a discussion on the settling of phytoplanktonic cells compared to inorganic particles). Sinking is mostly affected by hydrodynamics, but at the species-level, size, shape and colony-formation capacity are key determinants of the particle floatation. In this model, the sinking rate of each taxon is drawn from a beta distribution with a mean value of 9%, and a maximum around 30%, that is $s \sim 0.3\beta(0.55, 1.25)$ (see Fig. SXX), adapted from observations by Passow (1991) and Wiedmann *et al.* (2016).

Exchange rate The exchange rate between the ocean and the coast depends on the shape and location of the coast (estuary, cape, ...). At our calibration site (see section SXX), the renewal time ranges between 1 and 2.5 days (Ascione Kenov *et al.*, 2015), which corresponds to a daily rate between 40 and 100 %.

Cyst mortality and burial Cyst loss is the result of cyst mortality m and burial by sedimentation ζ . Mortality values range between 10^{-5} and 10^{-4} per day (more details on the approximation of mortality rates from McQuoid *et al.* (2002) are given in the SI). However, cyst burial by sedimentation might be a prevailing phenomenon in driving phytoplanktonic dynamics. Once cysts have been buried, they are not accessible for resuspension even if they could have germinated if put in an accessible location. Burial depends on the hydrodynamics of the site, but

also on biotic processes (i.e., bioturbation) and anthropogenic disturbances such as fishing or leisure activities (e.g., jet skiing). This parameter is thus heavily dependent on the environmental context and varies here between 0.001 and 0.1 per day.

Germination/resuspension Germination and resuspension are both needed for cyst to get back to the water column ($\gamma = \text{resuspension} \times \text{germination}$). Following McQuoid *et al.* (2002) and Agrawal (2009), we assume a temperature threshold: germination is triggered by temperatures going above 15°C. As actual rates of germination are not easily deduced from the literature, a set of credible values are tested (1%, 0.1%, 0.01%). Similarly, resuspension values are seldom computed for phytoplanktonic cells, but models for other particles such as sediments can be used. In this paper, we explore values between 10^{-5} (stratified water column) to 0.1 (highly mixed environment).

Parameter calibration

In addition to phenology parameters whose estimation process is described in the SI, the 49 non-null interactions that form the community matrix of the model are calibrated on field-data. These interactions are computed from previous models (Picoche & Barraquand, 2020, see SI for details on the equations) but need to be adjusted to take into account the differences in structure and time-step between studies.

The calibration procedure consisted in launching 1000 simulations, each characterized by a specific set of interaction coefficients. More precisely, for each simulation, each interaction coefficient (α_{ij} in model I, H_{ij} in model II) has the same probability of keeping its value, being increased or decreased by 10%, or being halved or doubled. The abundances of the coastal compartment are then extracted over the last 2 years of the simulation and compared to observations to compute the following summary statistics:

- average abundance $f_1 = \sqrt{\frac{1}{S} \sum_i^S (\bar{N}_{i,obs} - \bar{N}_{i,sim})^2}$ where S is the number of taxa.
- amplitude of the cycles $f_2 = \sqrt{\frac{1}{S} \sum_i^S [(\max(N_{i,obs}) - \min(N_{i,obs})) - (\max(N_{i,sim}) - \min(N_{i,sim}))]^2}$
- period of the bloom. The year is divided in 3 periods, i.e. summer, winter and the spring/autumn group (as taxa blooming in these periods can appear in either or both seasons). We give a score of 0 if the taxon blooms in the same period as its observed counterpart and 1 otherwise.

Simulations with taxon extinction are discarded. Models are ranked according to their performance for each summary statistic and the set of interactions with the best rank in every category is kept throughout the rest of the simulation.

Sensitivity analysis Certain parameters, which were evaluated from the literature, may be site- or model-specific, or vary over one order of magnitude, e.g. rates of sinking s , resuspension/germination γ , cyst mortality m and burial ζ , as well as the loss rate l . The dependence between variation in values and outputs of present models needs to be investigated before drawing conclusions for specific ecological scenarii. The set of tested values for each parameter is given in Table 1. Variations in average abundances and amplitudes at the community- and taxon levels for the last 2 years of simulations are the major model diagnostics.

Scenarii

Maintenance of biodiversity by exchanges between compartments can be gauged with two main scenarios:

1. modifying the storage by removing the cyst bank

2. changing the exchanges between the coast and the ocean ($e=0$)

Final richness and average abundance/biomass productivity (approximated by the final total abundances, to create a link with ecosystem functions) can be diagnostics.

We can make 2 a-priori ecological hypotheses. First, removing the cyst bank would increase the sensitivity to competition, i.e. decrease the maximum sustainable interspecific competition strength, and decrease the resilience of the community confronted to changes in the environment

Second, reducing the exchange with the ocean might lead to depletion of the ocean biomass and richness. In the ocean, individuals disappear through sinking and cannot reappear thanks to coastal production fueled by a cyst bank.

Results

Phytoplankton dynamics

Mean abundance of the various taxa was well reproduced and the phenology was overall reproduced as well. That said, in some cases abundances could be lower than expected and the variation in abundances due to seasonality was underestimated (Fig. 1).

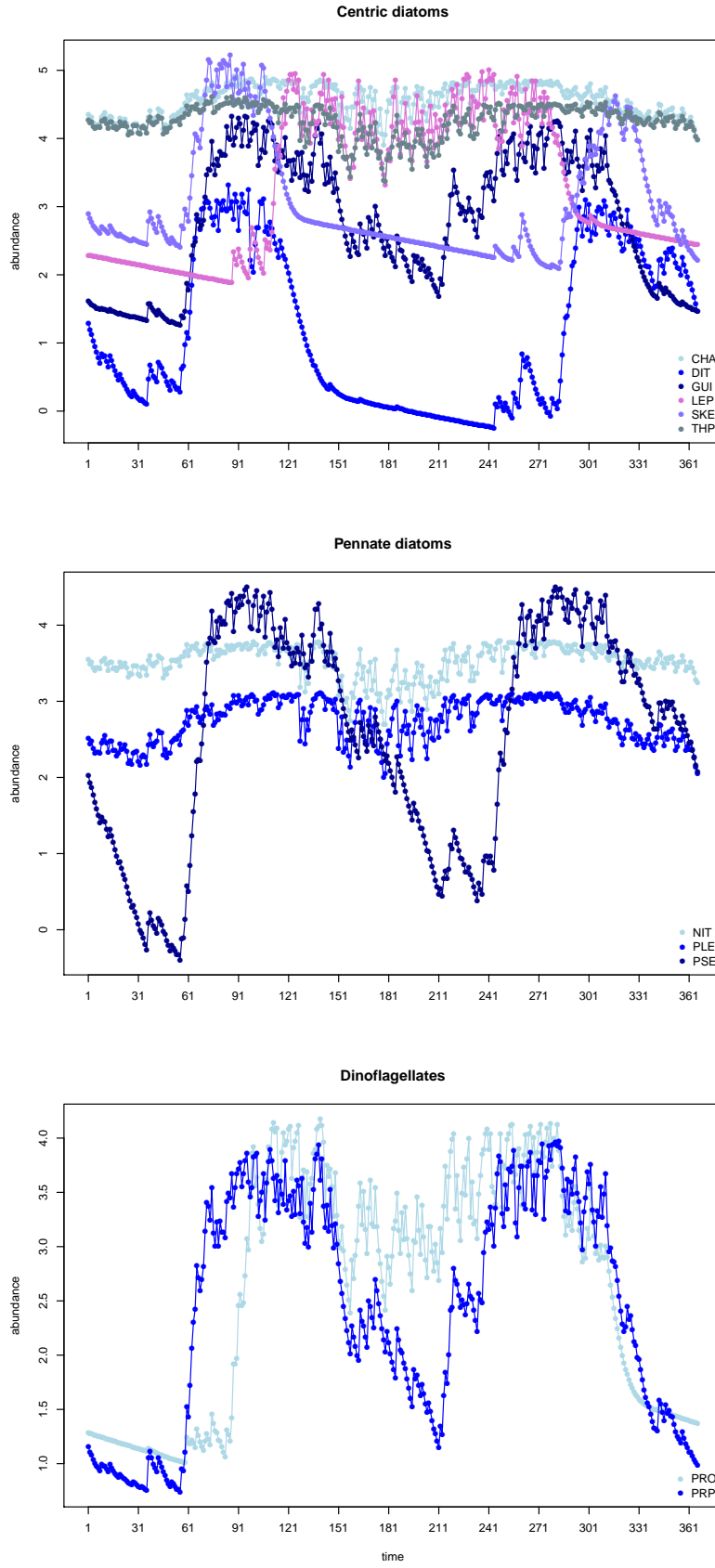


Figure 1: Simulated phytoplankton dynamics for a year in model I. Each panel corresponds to a cluster of interactions.

Sensitivity analysis to fixed parameter set

Total phytoplankton dynamics were not overwhelmingly affected by changes to other plausible values in the parameter set in both models (Fig. 2). The average change in abundance varied between -6.5 and 3% for model I and between -6 and 2% for model II. The range of abundance over a year, however, could be modified by -40 to 20%.

The change in abundance was most important with a decrease in mortality, while amplitudes were mostly affected by resuspension. Interestingly enough, while the vertical movement implied by the sinking and resuspension rates had similar effects on the amplitude (around $\pm 2\%$), the resuspension rate could lower the amplitude by nearly 40%.

In two cases, however, changes in parameters led to a loss of species: when cyst burial was increased (only 5 species remaining in the two models) and when resuspension was decreased (6 species remaining in model I, 7 species remaining model II). DIT, SKE, PRO and PRP always disappeared. GUI perished in all simulations, but the one with a decrease in resuspension in model II. LEP only went missing in model I, not in model II.

We can note that there is a trade-off between average change in abundance and average change in amplitude, as, most of the time, an increase in the first one led to a decrease in the second one.

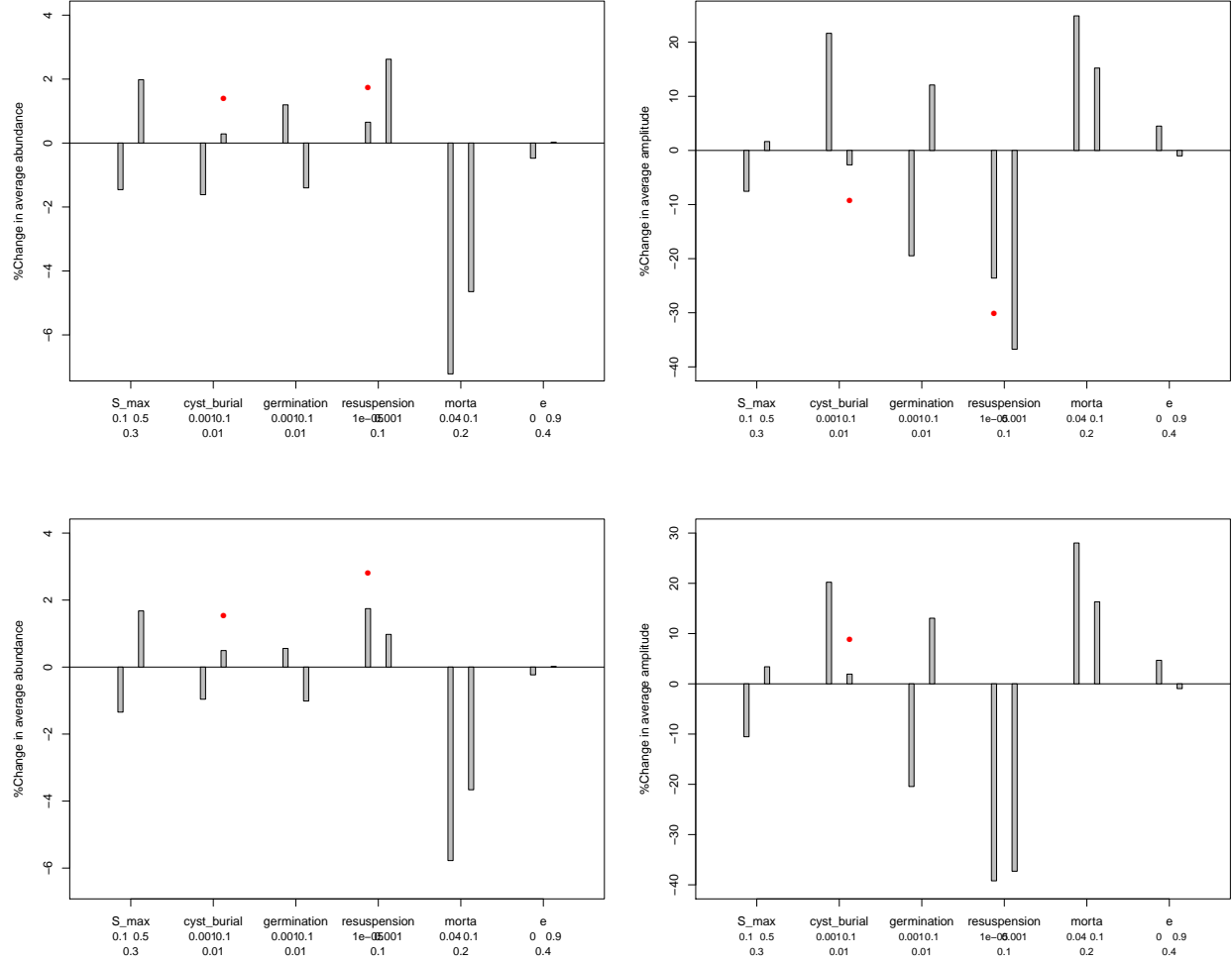


Figure 2: Sensitivity of the model to variation in parameters, measured as the mean difference in average abundance and amplitude of the coastal phytoplanktonic community in model I (top row) and model II (bottom row). Values used in all other simulations are in the third row of the x-axis while values tried in the sensitivity analysis are in the second row. Note that values used in the sensitivity analysis are not necessarily bounds around the usual values (i.e. tested mortality rates are both below the value used in other simulations). Red dots correspond to simulations in which at least one species disappeared. Variation in abundance with a maximum exchange rate cannot be seen as it is only 0.02%.

Finally, it appeared that the exchange rate, that is the flow of phytoplankton from the coast to the ocean, had a low, if not insignificant effect on the overall dynamics of the community.

Scenarios

Seed bank removal In both models, the removal of the seed bank significantly decreased the number of species in the community. DIT, LEP, SKE, GUI and PRP always disappeared.

Our first hypothesis was that the absence of the seed bank would cause the community to be less able to sustain competition. This proved to be only partially true as the relationship between richness and the strength of competition or facilitation was more of a dome-shaped one (Fig. 3). The relation was especially clear for model I, whose responses to a change in the interaction matrix were more stable: when competition was too high or facilitation was too low, the community richness decreased from 5 to 4. However, it should be noted that the poorer communities

(3 taxa) are a result of a lack of competition or an abundance of facilitation. In model II, this relationship is more complex. The community richness was decreased, even halved, in the presence of a seed bank when cumulated effects from other taxa were too low (competition too low or facilitation too high). When removing the seed bank, the community composition remains stable even for a large amount of competition. On the other hand, it reaches a peak in biodiversity when halving the competition strength, then decreases to an even lower richness.

In this context, facilitation and competition seem to play a nearly symmetric role, even though they are not present in the same proportions.

The abundance [[XXXX: For now, DRIVEN BY CHA]] of the total community, on the contrary, clearly decreases with competition strength in both models. [[We should investigate what happens for high facilitation in model I and even more in model II]]

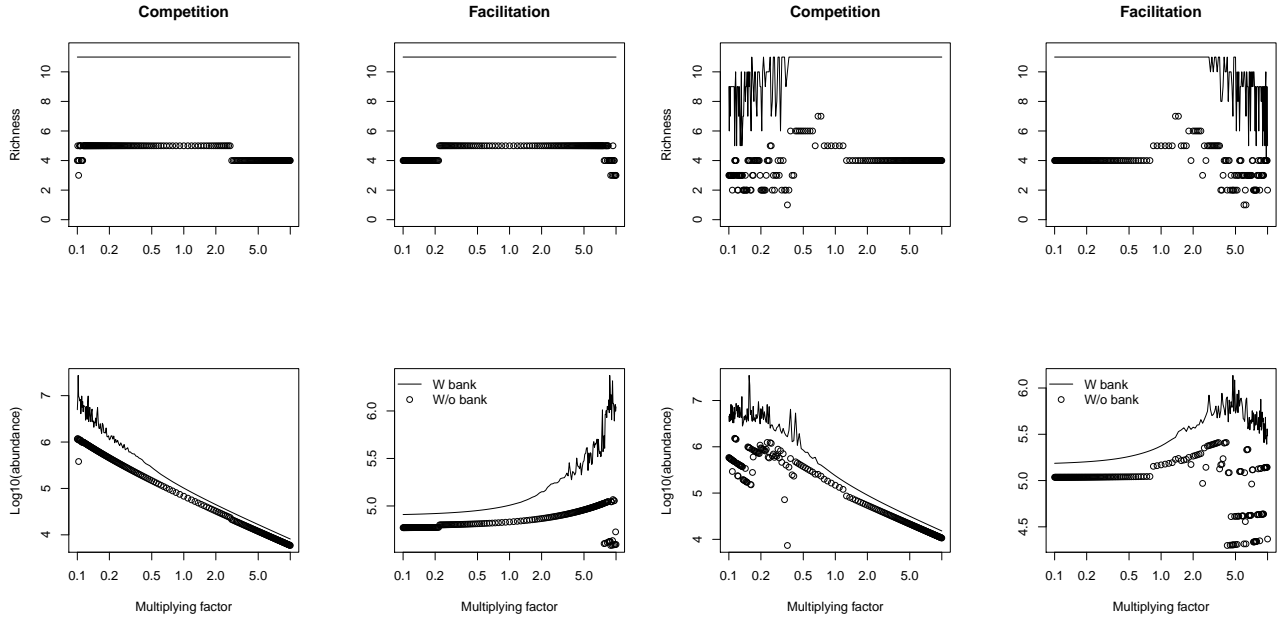


Figure 3: Variation in the total number of taxa still present at the end of the simulation (richness) and average total abundance with (line) and without (circles) a seed bank as a function of the strength of competition and facilitation for model I (left) and model II (right). The x-axis shows the factor by which each interaction was multiplied (note the logairthmic scale)

Species which disappear are always the same and can be related to the minimum abundance they can reach (Fig. 4).

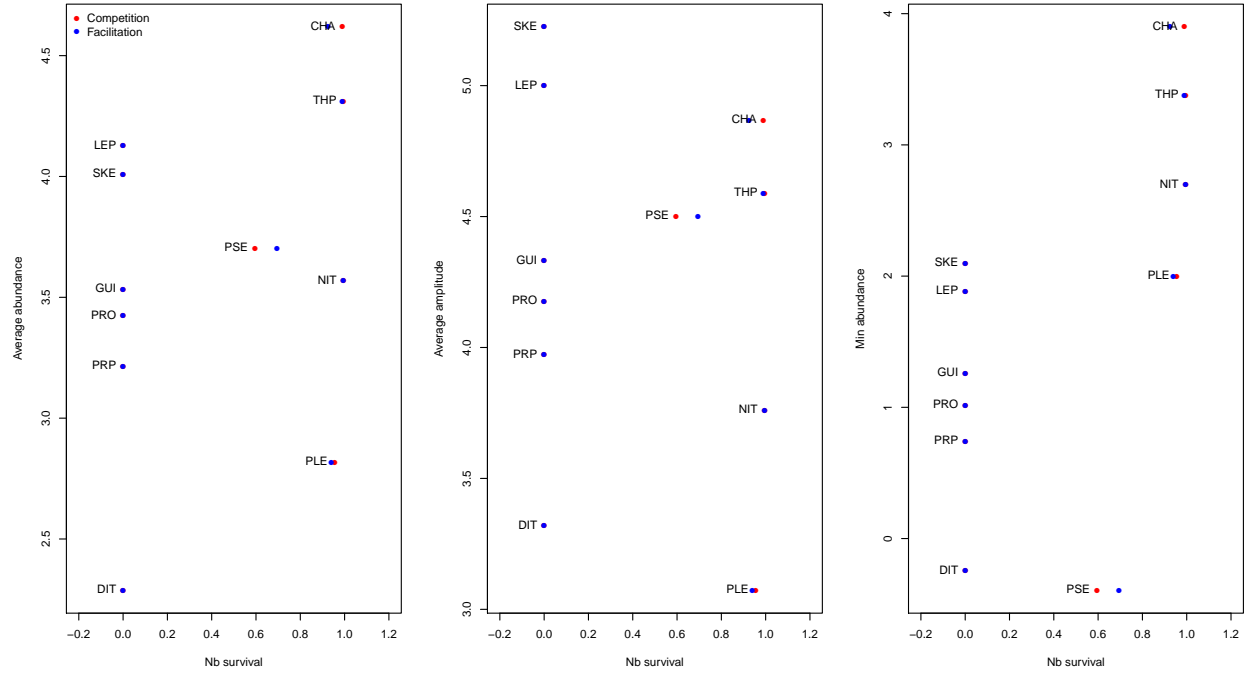


Figure 4: Probability of survival of species with variation in competition and facilitation as a function of their dynamics in the reference parameter set .

Our second hypothesis was that the absence of a seed bank would reduce the ability of a community to buffer changes in the environment, here represented as the temperature. As can be seen on Fig. 5, this was true for both models as the communities without seed bank could not remain with an increase in temperature above 2° , as opposed to communities with a seed bank which could only be affected by a 7°C increase (scenario SSP5 8.5). Even though the effects were less visible, a change (increase or decrease) in variance of the temperature also decreased the total number of species. In all cases however, the total abundances was not strongly affected.

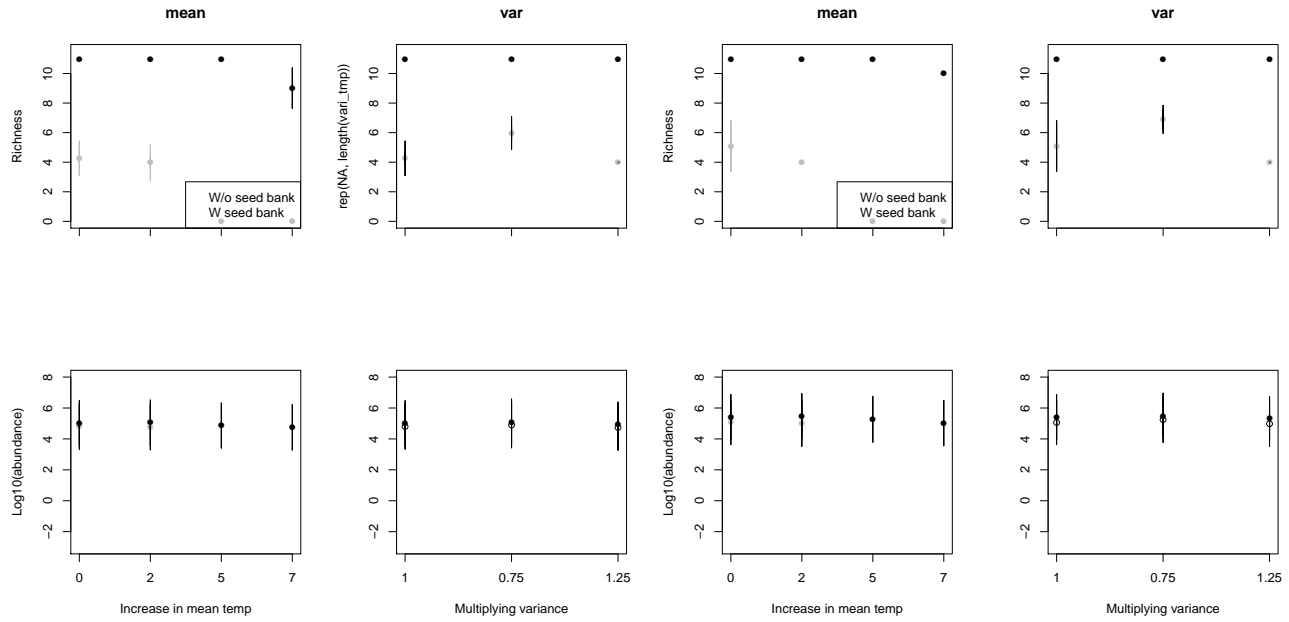


Figure 5: Variation in richness and total abundance with and without a seed bank as a function of the mean and variance of the temperature of competition and facilitation for model I (left) and model II (right).

Discussion

[[See outline]]

[[Need to compare our values to Jewson *et al.* (1981) who took into account most of the phenomena we describe here and the cyst bank as well as the water column]]

References

- Agrawal, S.C. (2009). Factors affecting spore germination in algae - review. *Folia Microbiologica*, 54, 273–302.
- Ascione Kenov, I., Muttin, F., Campbell, R., Fernandes, R., Campuzano, F., Machado, F., Franz, G. & Neves, R. (2015). Water fluxes and renewal rates at Pertuis d’Antioche/Marennes-Oléron Bay, France. *Estuarine, Coastal and Shelf Science*, 167, 32–44.
- Bissinger, J., Montagnes, D., Harples, J. & Atkinson, D. (2008). Predicting marine phytoplankton maximum growth rates from temperature: Improving on the Eppley curve using quantile regression. *Limnology and Oceanography*, 53, 487–493.
- Cáceres, C.E. (1997). Temporal variation, dormancy, and coexistence: A field test of the storage effect. *Proceedings of the National Academy of Sciences*, 94, 9171–9175.
- Chesson, P. (1986). Environmental variation and the coexistence of species. In: *Community ecology* (eds. Diamond, J. & Case, T.). Harper & Row, New-York, chap. 14, pp. 240–256.
- Comita, L., Queenborough, S., Murphy, S., Eck, J., Xu, K., Krishnadas, M., Beckman, N. & Zhu, Y. (2014). Testing predictions of the Janzen-Connell hypothesis: a meta-analysis of experimental evidence for distance- and density-dependent seed and seedling survival. *Journal of Ecology*, 102, 845–856.

- Ellegaard, M. & Ribeiro, S. (2018). The long-term persistence of phytoplankton resting stages in aquatic seed banks'. *Biological Reviews*, 93, 166–183.
- Ellner, S., Snyder, R. & Adler, P. (2016). How to quantify the temporal storage effect using simulations instead of math. *Ecology Letters*, 19, 1333–1342.
- Eppley, R. (1972). Temperature and phytoplankton growth in the sea. *Fishery Bulletin*, 70, 1063–1085.
- Hinners, J., Hense, I. & Kremp, A. (2019). Modelling phytoplankton adaptation to global warming based on resurrection experiments. *Ecological Modelling*, 400, 27–33.
- Jewson, D.H., Rippey, B.H. & Gilmore, W.K. (1981). Loss rates from sedimentation, parasitism, and grazing during the growth, nutrient limitation, and dormancy of a diatom crop. *Limnology and Oceanography*, 26, 1045–1056.
- Marcus, N. & Boero, F. (1998). Minireview: The importance of benthic-pelagic coupling and the forgotten role of life cycles in coastal aquatic systems. *Limnology and Oceanography*, 43, 763–768.
- McQuoid, M.R., Godhe, A. & Nordberg, K. (2002). Viability of phytoplankton resting stages in the sediments of a coastal Swedish fjord. *European Journal Phycology*, 37, 191–201.
- Nguyen, V., Buckley, Y.M., Salguero-Gómez, R. & Wardle, G.M. (2019). Consequences of neglecting cryptic life stages from demographic models. *Ecological Modelling*, 408, 108723.
- Passow, U. (1991). Species-specific sedimentation and sinking velocities of diatoms. *Marine Biology*, 108, 449–455.
- Patrick, R. (1948). Factors effecting the distribution of diatoms. *Botanical Review*, 14, 473–524.
- Picoche, C. & Barraquand, F. (2020). Strong self-regulation and widespread facilitative interactions between genera of phytoplankton. preprint, bioRxiv.
- Qian, J. & Akçay, E. (2020). The balance of interaction types determines the assembly and stability of ecological communities. *Nature Ecology & Evolution*, 4, 356–365.
- Reynolds, C.S. (2006). *The ecology of phytoplankton*. Cambridge University Press.
- Sanyal, A., Larsson, J., van Wirdum, F., Andrén, T., Moros, M., Lönn, M. & Andrén, E. (2018). Not dead yet: Diatom resting spores can survive in nature for several millennia. preprint, bioRxiv.
- Scranton, K. & Vasseur, D.A. (2016). Coexistence and emergent neutrality generate synchrony among competitors in fluctuating environments. *Theoretical Ecology*, 9, 353–363.
- Shoemaker, L.G. & Melbourne, B.A. (2016). Linking metacommunity paradigms to spatial coexistence mechanisms. *Ecology*, 97, 2436–2446.
- Smayda, T.J. (2002). Turbulence, watermass stratification and harmful algal blooms: an alternative view and frontal zones as “pelagic seed banks”. *Harmful Algae*, 1, 95–112.
- Wiedmann, I., Reigstad, M., Marquardt, M., Vader, A. & Gabrielsen, T. (2016). Seasonality of vertical flux and sinking particle characteristics in an ice-free high arctic fjord-Different from subarctic fjords? *Journal of Marine Systems*, 154, 192–205.
- Wisnoski, N.I., Leibold, M.A. & Lennon, J.T. (2019). Dormancy in metacommunities. *The American Naturalist*, 194, 135–151.